EXPERIMENTAL INVESTIGATION ON THE MOMENT-ROTATION PERFORMANCE OF PULTRUDED GFRP WEB-FLANGE JUNCTIONS

Gisele Góes Cintra
Daniel C. T. Cardoso
giseleg.cintra@aluno.puc-rio.br
dctcardoso@puc-rio.br
Pontifical Catholic University of Rio de Janeiro (PUC-Rio)
Rua Marquês de São Vicente, 225, 22451-900, Rio de Janeiro - RJ, Brazil
Janine D. Vieira
janinedv@id.uff.br
Fluminense Federal University
Rua Passo da Pátria, 156, 24210-240, Niterói - RJ, Brazil.

Abstract. This paper aims to present an experimental investigation on the rotational stiffness of pultruded glass-fiber reinforced polymer (pGFRP) cross-section junctions. Channels and I-sections with different types of resins were studied and a novel set-up was developed to experimentally characterize the junctions in a direct manner. The digital image correlation (DIC) technique was used to monitor deflections and angles of rotation, as well as the cracks formation. In addition, fiber architecture was analyzed through an optical microscope and correlated with the moment-rotation response.

Keywords: GFRP; Rotational stiffness; Web-flange junction; Digital image correlation (DIC).

1   Introduction

The use of pultruded glass-fiber reinforced polymer (pGFRP) in structural applications has greatly increased in the past few decades, due to their several advantages over traditional materials, such as its lightweight, corrosion resistance and ability to tailor geometry. Researches worldwide have dedicated significant efforts to better understand the material performance, especially when it comes to instability problems.

In this scenario, the behavior of the junctions between adjacent plates comprising the cross section became a matter of interest due to its influence on the buckling response of pultruded members. The local failure at these regions affects the overall structure behavior, having influence on stiffness and ultimate limit state [1]. Previous works [2–4] have shown that web-flange junctions (WFJs) are characterized by a semi-rigid constitutive behavior, which affects the local buckling loads [5].

It is well known that the composites failure is often related to the junctions, which are considered the weakest zone by some authors due to its complex fiber architecture and resin-rich zones [1,6-8]. Because of the particular fiber arrangement, the WFJs mechanical properties are different from the flat regions of the profile, making the junctions characterization a topic of great relevance. In this context, many authors have devoted attention to develop appropriate techniques to determine the moment-rotation relations ($M - \theta$) [2,3,9-13], but these are either determined indirectly or directly but requiring special apparatus. Failure modes related to delamination at the triangular core rovings are usually reported.

Based on the researches available on literature, the present authors have identified the need of characterize the rotational stiffness through a simple and adaptable set-up, which will be presented in the following sections. The parameters determined herein may, then, be used in numerical models where junction properties can be incorporated.

2   Ongoing Experimental Program

An ongoing experimental program intending to investigate the WFJ's rotational stiffness has been conducted. In all, twelve specimens extracted from three different cross-sections were analyzed using Digital Image Correlation (DIC) [7].

2.1 Developed set-up

The test set-up used for characterization of WFJs rotational stiffness is shown in Figure 1. Specimens were clamped to a steel angle using rigid aluminum bars and screws. The steel angle, on the other hand, was attached to a base, preventing the specimens from coming out of the load application plane. This configuration allows the set-up to be adapted to different cross-sections. The load *P* was applied through a roller to the specimens' stem at a distance d of the web-flange junction, as shown in Figure 2.
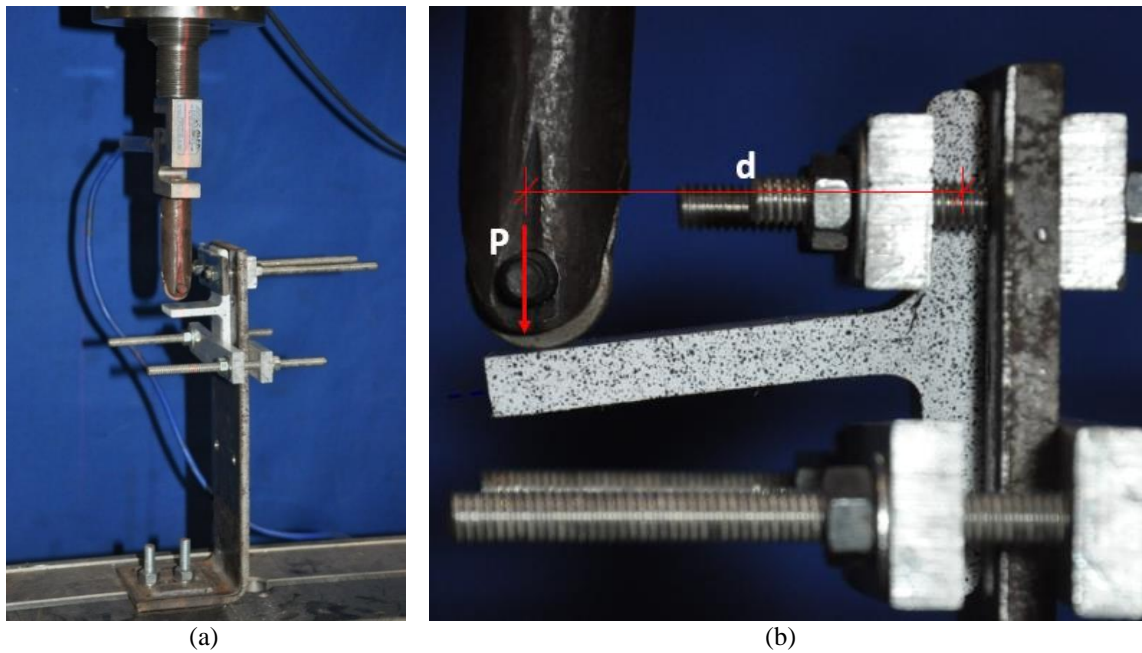
Figure 1. Test set-up: (a) Overview; (b) detail of the test configuration

To measure the displacements δ and the web's angle of rotation about the junction θ, photos were taken every five seconds with a *Nikon D90* and were subsequently analyzed in the free software *GOM Correlate 2017* [8]. Through the moment applied $M=P$ x d and the rotation θ, the rotational stiffness k_r is obtained directly as the slope of the plot *M versus θ*. All tests were conducted under displacement control at a rate of 0.6 mm/min until failure using a servo-hydraulic universal testing machine *MTS 244.41* with a load capacity of 500 kN. Once the machine load capacity was much higher than the specimens ultimate load, a load cell of 2.5 kN capacity was used.

I-sections and channels, with dimensions of 101.6 x 101.6 x 6.4-mm and 152.4 x 41.28 x 5-mm, respectively, made with E-glass fibers and vinyl ester resin were used in the study. Twelve specimens having 35-mm wide were extracted from both sections and tested, among which four were extracted from the I-sections and eight from the channels, as shown in Figure 2.
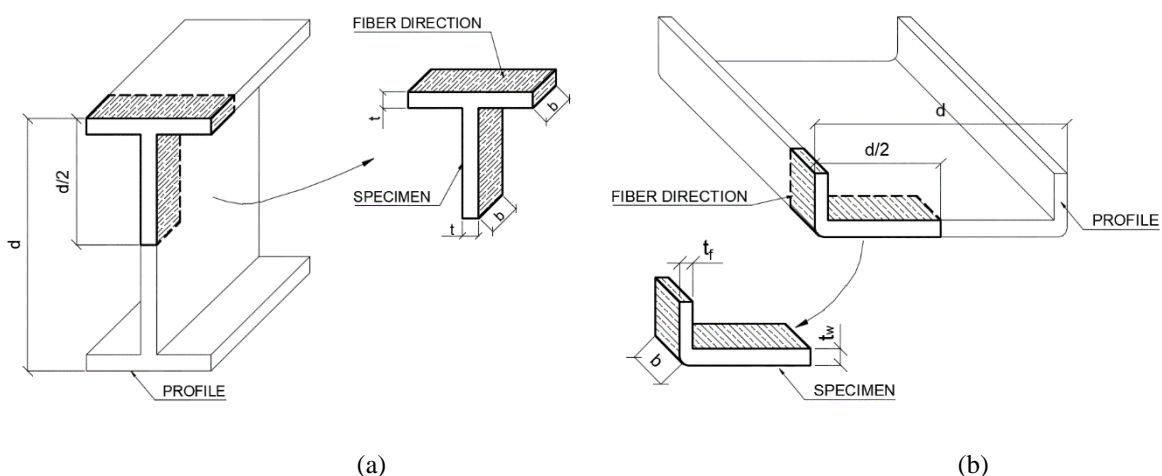
Figure 2. Specimens extracted from profiles: (a) from I-section profiles; (b) from channels.

For the specimens extracted from channel, four were positioned in order that the applied load caused a 'section closure' during the test, whereas the other four were loaded in order to 'open' the

section, as presented in Figure 3. This procedure was adopted once different behavior were reported in literature [1] for close- and open-modes. The web's angle of rotation about the junction was measured directly through the software GOM, having the undeformed shape as a reference. To validate the results, displacements obtained using GOM software were compared with those obtained using a displacement transducers.

(a)	(b)
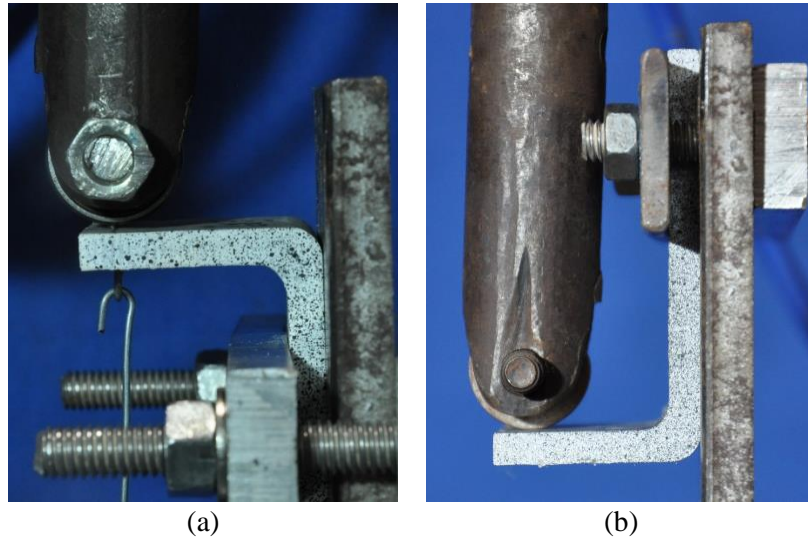
Figure 3. Channel section tests: (a) close-mode; (b) open-mode

2.2 Results and Discussion

The results were plotted in moment (*M*) *versus* rotation (*θ*) curves, which are presented in Figures 4 (I-sections) and 5 (Channels). The rotational spring constants can be obtained by dividing the curve slope at linear range for the specimen width and their average values are shown in Tables 1 to 3.
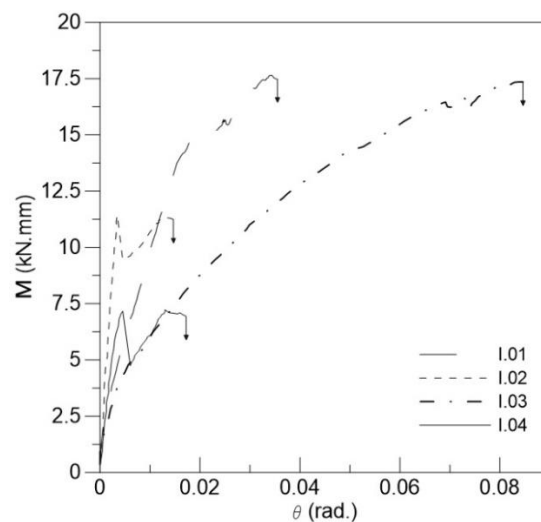
Figure 4. *Mxθ* curve of specimens extracted from I-sections.
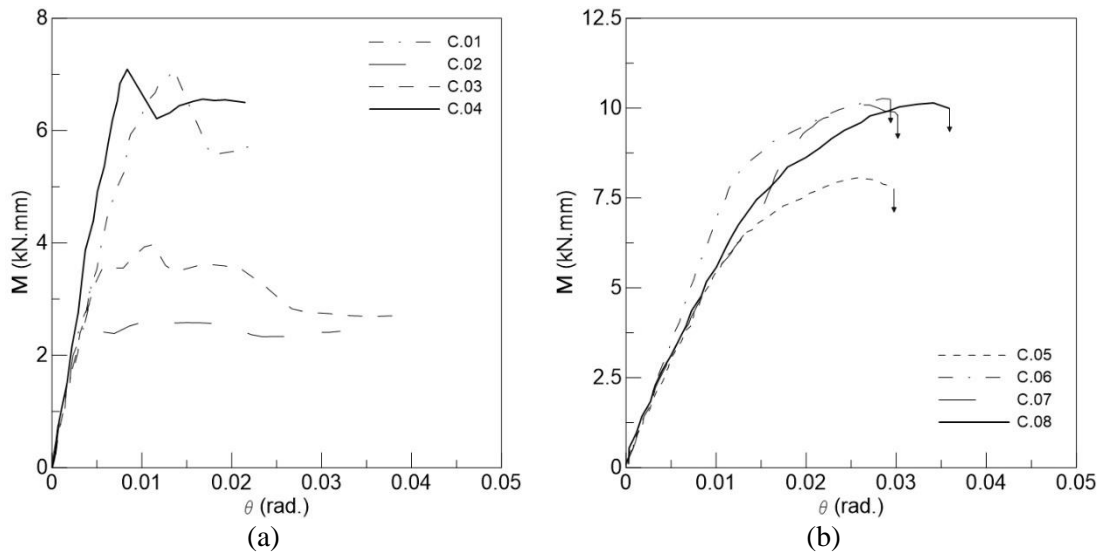
Figure 5. *Mxθ* curve of specimens extracted from channel sections: (a) open mode; (b) closed mode.

Table 1. Average Rotational Stiffness k_r for I1-section.

Specimen	k_r (kN/rad)
I.01	92.03
I.02	94.94
I.03	22.73
I.04	56.27
Average	**66.49 (0.44)**

Table 2. Average rotational stiffness k_r for channels (open mode).

Specimen	k_r (kN/rad)
C.01	16.95
C.02	19.65
C.03	17.84
C.04	23.97
Average	**19.60 (0.13)**

Table 3. Average rotational stiffness k_r for channels (closed mode).

Specimen	k_r (kN/rad)
C.07	15.48
C.08	18.33
C.09	15.17
C.10	14.98
Average	**15.99 (0.08)**

In the same way that was observed in literature, the average results for I-sections WFJS rotational stiffness presents a great variability and this may be explained by the complexity of fiber architecture in the junction region. The channels, on the other hand, presented lower values for rotational stiffness when compared to I-sections, with lower variability of results. For channel sections, although the junction stiffness is similar for both tested configurations, there is a clear difference in the overall behavior of the channel junctions, as shown in Figure 5, which is associated to the different stress trajectories experienced by the pGFRP layers in each case.

In order to better understand the influence of the fiber arrangement at the region and also on the cracks pattern, pictures were taken before and after failure with the aid of a *Nikon SMZ 800* optical microscope. It can be observed in Figures 6a and 6b that cracks for I-sections are formed on the mat region for both sections, following the same pattern reported by Turvey and Zhang [9] – called *"delamination"* by the authors. It is important to highlight that this delamination is produced by tensile stress perpendicular to the mat surface, therefore separating the layers in a porous zone. Cracks in regions where mat was wrinkled could also be observed, especially in tension zones. For channel sections the fiber architecture is more uniform, with lower incidence of mat wrinkling due to its junction's shape.

(a)   (b)

(c)   (d)
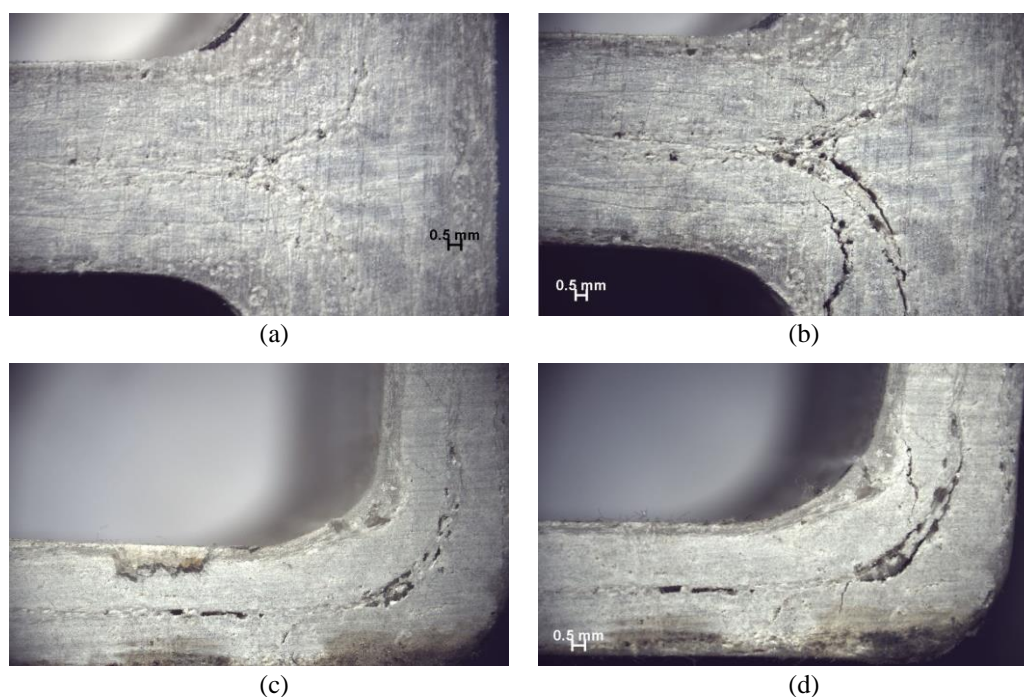
Figure 6. Specimens delamination: (a) I-section before testing; (b) I-section after testing; (c) channel before testing; (d) channel after testing.

Conclusions

A simple set-up was developed to characterize the rotational stiffness of WFJs of pultruded GFRP. The parameter may be determined through the moment *versus* angle of rotation curve with the aid of the DIC technique. Thus, the stiffness is obtained by direct means, since the angle of rotation can be easily determined through the GOM software.

The results of this ongoing experimental program have shown that the I-sections presented higher values for k_r, with a greater variability in results when compared to specimens extracted from channels. This may be explained by the more incidence of mat wrinkling and consequently, due to a lack of pattern for the fiber architecture in this region. The common presence of resin-rich zones in I-section junctions may also have affected the results.

The specimens extracted from channels were loaded in closed and open modes. Although no significant differences have been observed on values of k_r when comparing both modes, the overall behavior of each junction has changed from one mode to another.

Finally, the mode failure for the two studied cross-sections were similar to those observed in literature, with cracks formation on the mat region.

Acknowledgements

References

[1]   Mosallam AS, Feo L, Elsadek A, Pul S, Penna R. Structural evaluation of axial and rotational flexibility and strength of web-flange junctions of open-web pultruded composites. Compos Part B Eng 2014;66:311–27. doi:10.1016/j.compositesb.2014.05.018.

[2]   Yanes-Armas S, de Castro J, Keller T. Rotational stiffness of web-flange junctions of pultruded GFRP decks. Eng Struct 2017;140:373–89. doi:10.1016/j.engstruct.2017.03.003.

[3]   Turvey GJ, Zhang Y. A computational and experimental analysis of the buckling, postbuckling and initial failure of pultruded GRP columns. Comput Struct 2006;84:1527–37. doi:10.1016/j.compstruc.2006.01.028.

[4]   Ascione L, Berardi VP, Giordano A, Spadea S. Local buckling behavior of FRP thin-walled beams: A mechanical model. Compos Struct 2013;98:111–20. doi:10.1016/j.compstruct.2012.10.049.

[5]   Turvey GJ, Zhang Y. Shear Failure Strength Of Web-Flange Junctions In Pultruded GRP Profiles. Adv Polym Compos Struct Appl Constr ACIC 2004 2004;36:553–60. doi:10.1016/B978-1-85573-736-5.50062-5.

[6]   Turvey GJ, Zhang Y. Tearing failure of web-flange junctions in pultruded GRP profiles. Compos Part A Appl Sci Manuf 2005;36:309–17. doi:10.1016/j.compositesa.2004.06.009.

[7]   Sause MGR. Digital image correlation. Springer Ser Mater Sci 2016;242:57–129. doi:10.1007/978-3-319-30954-5_3.

[8]   GOM Correlate. Evaluation Software for 3D Testing n.d. https://www.gom-correlate.com/ (accessed February 11, 2018).

[9]   Turvey GJ, Zhang Y. Characterisation of the rotational stiffness and strength of web-flange junctions of pultruded GRP WF-sections via web bending tests. Compos Part A Appl Sci Manuf 2006;37:152–64. doi:10.1016/j.compositesa.2005.04.022.